

**Master of Science Thesis in Medical Physics**

# Monte Carlo dose simulation

-of chest and hip joint tomosynthesis

**Johan Tano**

**Supervisors:**

Magnus Båth

Angelica Svalkvist

Department of Radiation Physics

University of Gothenburg

Gothenburg, Sweden

August 2014



UNIVERSITY OF GOTHENBURG

The Sahlgrenska Academy

## Abstract

The purpose of the present work was to determine the conversion factor between kerma-area product (KAP) and effective dose for a chest tomosynthesis examination of different patient sizes and tube voltages for the clinical system GE Definium 8000 with the chest tomosynthesis option VolumeRAD, according to both ICRP 103 and ICRP 60. Also investigated was the total effective dose of a hip joint examination. The program used for simulation was PCXMC 2.0, which is a Monte Carlo based program developed by STUK (Radiation and Nuclear Safety Authority in Finland). The average conversion factor between KAP and effective dose was calculated for different patient sizes, ranging from 0.386 mSv Gy<sup>-1</sup> cm<sup>-2</sup> for a thin patient (170 cm/50 kg) to 0.217 mSv Gy<sup>-1</sup> cm<sup>-2</sup> for an obese patient (170 cm/100 kg). The different tube voltages gave conversion factors ranging from 0.612 mSv Gy<sup>-1</sup> cm<sup>-2</sup> for 60 kV to 0.326 mSv Gy<sup>-1</sup> cm<sup>-2</sup> for 150 kV for a standard patient (170 cm/70 kg). The total effective dose of a hip joint examination was determined to be 0.86 mSv which is 9.5 times that of a dose from a conventional PA radiography.

## Table of contents

Introduction.....	4
Background.....	4
Tomosynthesis examination and system .....	4
Earlier work .....	6
Purpose of the present work.....	6
Materials and Method.....	7
PCXMC software .....	7
International Commission on Radiological Protection (ICRP) .....	7
Simulation and Calculation.....	8
Chest.....	9
Hip Joint.....	10
Results .....	11
Discussion .....	12
Conclusion .....	14
Acknowledgements .....	15
References.....	15

# Introduction

## Background

Tomosynthesis refers to the technique of acquiring multiple radiographs over a limited angular range and using these radiographs to reconstruct slices of the imaged object (1). The development of tomosynthesis has been described by Dobbins et al (2, 3, 4). The concept of tomosynthesis existed decades before it could be used practically. In the 1930s the basic theoretical framework for limited angle tomography was provided by Ziedses des Plantes (5). The term “tomosynthesis” first appeared in 1972 in a paper by Grant (6) that described the method of tomosynthesis reconstruction. A difficulty that all early methods encountered was the residual blur from objects outside the plane of interest, but in the mid 1980s a number of studies were successful in finding methods that decreased the blur from overlying anatomy (e.g. 7, 8). With the deblurring algorithms soft-tissue anatomy of interest was depicted clearer and tomosynthesis was made more suitable for a wider range of clinical applications. Research however came to a halt in the late 1980s and for about a decade onwards, due to the introduction of the spiral CT. This situation changed substantially in the late 1990s, with the introduction of the flat panel radiographic detector, as there was finally a device that could image at the speed necessary for reasonable use in tomosynthesis. One of the early applications of tomosynthesis was in chest imaging, primarily for pulmonary nodule imaging (9).

Different types of tomosynthesis implementations have been described over the years (e.g. 10,11). Clinical uses of tomosynthesis have included vascular imaging (12), dental imaging (13), orthopedic imaging (e.g. 14, 15), mammographic imaging (16) and chest imaging (17). Several technological advances within the past decades have contributed to making tomosynthesis clinically practical (4). The most important advance, as described by Dobbins and McAdams (4), has been the development of flat-panel detectors, as mentioned earlier. The important qualities that these detectors have are high detective quantum efficiency, few artifacts and the fact that they are self-scanned at a rate suitable for rapid image acquisition needed for tomosynthesis. Some of the other key technological developments that have made tomosynthesis work possible are improved deblurring algorithms, to suppress blur from out of plane objects (e.g. 18, 19), and increased computer speed that makes it possible to have a reconstruction time suitable for clinical use.(4)

## Tomosynthesis examination and system

Figure 1 depicts a prototype setup for a chest tomosynthesis system described by Dobbins and McAdams (4). The patient is positioned in front of a stationary flat panel detector, and a general scout image is taken, also referred to as the zero degree projection. The purpose of the scout is to be certain that the field of view is placed correctly. In the prototype created by Dobbins and McAdams a motorized tube crane causes the X-ray tube to motion in a vertical path as images are taken rapidly during the tube movement. The images are recorded in coordination with the X-ray generator and a computer is used to control the movement of the X-ray tube. Two linear actuators are used to move the tube vertically and rotate it about an axis so that it always is facing the center of the detector during its vertical motion, i.e. the point of rotation. A computer is then also used to reconstruct the tomosynthesis section images. (3).

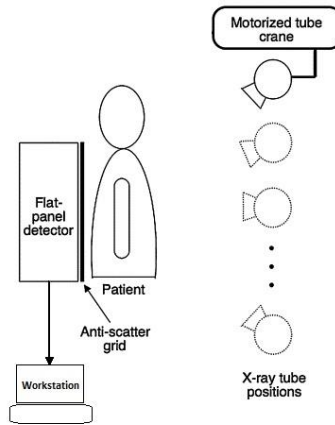


Figure 1 A simplified drawing of the motion of the X-ray tube (modified (4))

The projection images collected are then reconstructed to create section images. The first step in the reconstruction of the section images is to perform a simple shift-and-add computation, equivalent to a simple back projection, to generate conventional tomosynthesis images. Figure 2 demonstrates how the shift-and-add method works. In the patient depicted in fig. 2, the plane of interest contains a triangle and the circle is the plane of overlying anatomy that is to be avoided. With a conventional radiography there would be no way to avoid the circles and the triangles would be obscured. Five projection images are acquired in this example, the circle and triangle are projected onto different places in the imaging detector based on their relative height above the detector and the distance between tube locations. These five images can then be shifted in such a way that the triangles all line up and the circles are spread out and therefore blurred into the background. Now we have an image depicting the plane of interest without the troubling overlying anatomy. By changing how the images are shifted in relation to each other, a different plane can of course be generated, so that instead of focusing on the triangles the circles could be lined up and the triangles spread giving a slice image of the circles instead. A series of tomosynthesis slice images throughout the entire volume of the patient could also be generated (4).

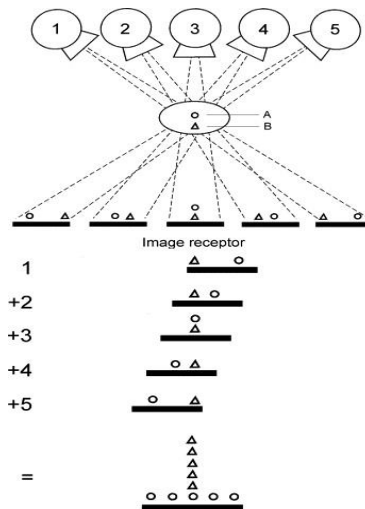


Figure 2 A simplified example of the shift-and-add technique (modified (2))

A commercially available chest tomosynthesis system is the GE Definium 8000 system with VolumeRAD option (GE Healthcare, Chalfont St. Giles, UK), as described in depth by Svalkvist (1). To determine the total exposure for a tomosynthesis examination a scout image of the patient is acquired using automatic exposure control (AEC). Total exposure is calculated by the software by multiplying the tube load (mA s) used for the scout image by a factor, with the factor most commonly used being 10. The total mA s calculated is then spread evenly over the 60 projections that constitute a tomosynthesis examination (1).

## **Earlier work**

Diagnostic imaging of the chest is made difficult by the many different types of diseases encountered. Radiographic evaluation of the chest can be used to evaluate nodular disease, airway disease and diffuse interstitial disease, placement of tubes and lines, and structures of the mediastinum or spine (2). Diagnostic prognosis is often made difficult due to overlying anatomy. In clinical situations today this problem can be solved using computer tomography (CT) or tomosynthesis. Tomosynthesis, even if it does not have the depth resolution of CT, has other practical advantages. With very small changes to a conventional digital chest imaging room, it is possible to produce tomosynthesis images at about the same time as a conventional chest exam. This could possibly give a reduction in the amount of CT scans, which could result in lowering both cost and radiation dose (4). The effective dose from a chest tomosynthesis examination in a study at the University of Gothenburg (20) indicated that the effective dose is 0.13 mSv, which is only about 2 % of an average chest CT, but approximately two to three times the effective dose of a conventional radiography examination (20). This however was an average dose to patients with weights varying between 60 to 80 kg (average 70.2 kg), and hence does not indicate how the dose changes with increasing or decreasing patient size and weight, or the effects of tube voltage. There have been previous investigations by Svalkvist et al. of dose correlation with patient size (21), but not on the clinically used system GE Definium 8000. Studies on the change of dose to patient of different tube voltages also have not been performed on the clinical system, however Svalkvist et al. (21) studied these effects on a fictive system, calculating the conversion factor. Conversion factors are used to easily enable an estimation of the effective dose for a certain radiological procedure. The concept was introduced by the UK National Radiological Protection Board (NRPB) in 1994 (1) and the conversion factor is related to a exposure unit acquired in a clinical examination, for example the kerma area product (KAP) as is used for the conversion factor in the paper by Svalkvist et al. (21). In that paper the conversion factors related to the kerma area product ( $\text{mSv Gy}^{-1} \text{cm}^{-2}$ ) ranged from 0.37  $\text{mSv Gy}^{-1} \text{cm}^{-2}$  for the smallest patient (170 cm, 50 kg) to 0.21  $\text{mSv Gy}^{-1} \text{cm}^{-2}$  for the most obese patient (170 cm, 100 kg). The conversion factor for different tube voltages ranged from 0.26  $\text{mSv Gy}^{-1} \text{cm}^{-2}$  for 100 kV to 0.31  $\text{mSv Gy}^{-1} \text{cm}^{-2}$  for 150 kV for a standard patient (170 cm, 70 kg).

## **Purpose of the present work**

The main purpose of the present work was to determine the conversion factor between KAP and effective dose for a chest tomosynthesis examination for different patient sizes and tube voltages for the clinical system GE Definium 8000, using weighting factor from both ICRP 103 (22) and ICRP 60 (23). This was performed by simulation using PCXMC 2.0. An additional purpose was to investigate another clinical application for which tomosynthesis is well suited, that is the imaging of joints. This has been clinically used at Sahlgrenska University Hospital Mölndal, Gothenburg, Sweden, for many

types of joints, such as hand, shoulders, knees and hip joints. From a dose standpoint radiation to extremities is not as dangerous due to the fact that there are no vital organs in the field of view. However in imaging of the hip joint many radiation sensitive organs (22) come into view, and due to this it is important to investigate the dose received from a hip joint examination. The purpose of the hip joint study was to determine the effective dose and conversion factor of a hip joint tomosynthesis examination and determine the effective dose of a conventional radiography examination.

## **Materials and Method**

### **PCXMC software**

The PCXMC software is a Monte Carlo based program (24) developed by the Radiation and Nuclear Safety Authority in Finland (STUK), and is a well tested way to investigate the dosimetry of a chest tomosynthesis system (20, 21, 25). The program was used in order to simulate projections from different angles and calculating the resulting effective doses from these projections. The PCXMC version 2.0 used in this study calculates both organ doses and resulting effective doses using anatomical data from mathematical phantom models. The version 2.0 gives doses both according to ICRP 60 and ICRP 103. In the program both phantom height and weight can be adjusted, which makes it possible to investigate different patient sizes. The geometry in the program for the X-ray projections can be adjusted using the given parameters of conventional systems. In this rapport PCXMC was used to simulate the Definium 8000 system by having the same focus detector distance (FDD), incident angles of the central axis of the tube ray and location of the reference point, through which the central axis of the X-ray beam rotates. In the case of a tomosynthesis examination, each projection must be separately handled, while the resulting effective dose of the entire examination is obtained by summation of the contributions from each projection angle. The photon transport through the patient depends on a mathematical probability distribution of all possible interaction processes. By specifying the number of photons used in the simulation the Monte Carlo uncertainty can be determined. In the present work,  $1.8 \times 10^7$  photon histories were used for each scout, and  $3 \times 10^5$  photon histories were used for each of the 60 projections of the tomosynthesis, resulting in total of  $1.8 \times 10^7$  photons for the entire acquisition. The resulting uncertainty for the Monte Carlo simulation was <0.1%. For the dose calculation both the characteristics of the desired X-ray spectrum such as tube voltage, anode angle and filtration is selected and the exposure measure is entered, and in this paper KAP and mA s (current-time product) were used. Between the different projections the current-time product was evenly distributed.

### **International Commission on Radiological Protection (ICRP)**

The first ICRP recommendations, which intended to protect medical professionals against occupational exposure, were published in 1928 (26). General recommendations have thereafter been updated and recommendations in new fields have been given. The ICRP is based on the approach that stochastic effects have a linear-no-threshold (LNT) dose response. The ICRP's new recommendations issued in 2007 had the purpose of simplifying the advice and to strengthen the general principles that were featured in ICRP 60. In table 1 the weight factors of ICRP 103 and ICRP 60 for different organs and tissues are shown. In ICRP 103 the organs which are not listed are grouped together and called remainder organs which has a combined value of 0.12, that is shared among 14 organs, though only 13 for each sex, which are adrenals, extrathoracic tissue, bladder, heart, kidneys, lymphatic nodes, muscle, oral mucosa, pancreas, prostate (male), small intestine ,

spleen, thymus, and uterus (female). In ICRP 60 the remainder organs are all given the combined value of 0.05 and these organs are; adrenals, brain, small intestine, kidney, muscle, pancreas, spleen, thymus, uterus (22, 23).

**Table 1 weight factor for organs and tissues for both ICRP 103 and ICRP 60 (values from (22, 23))**

Organ/Tissue	Weight Factor $w$	
	ICRP 103	ICRP 60
Breast	0.12	0.05
Bone marrow	0.12	0.12
Colon	0.12	0.12
Lung	0.12	0.12
Stomach	0.12	0.12
Gonads	0.08	0.20
Bladder	0.04	0.05
Liver	0.04	0.05
Oesophagus	0.04	0.05
Thyroid	0.04	0.05
Bone surfaces	0.01	0.01
Brain	0.01	-
Salivary glands	0.01	-
Skin	0.01	0.01
Remainder organs	0.12	0.05

## Simulation and Calculation

The field sizes for all projections are, by the tomosynthesis system, defined at the detector surface, but in PCXMC 2.0 the field sizes are defined where the radiation enters the patient, so the field sizes were recalculated for the patient skin. This was done using eq. 1, where  $x_{PCXMC,i}$  is the field size that was used in the program,  $FSD_i$  is the focus to skin distance,  $FDD_i$  is the focus detector distance and  $x_i$  is the field size at the detector surface.

$$x_{PCXMC,i} = x_i \times \frac{FSD_i}{FDD_i} \quad \text{Eq. 1}$$

The focus to skin distance was calculated by using the FDD of the system and measuring the patient thickness in the program and adding a 5 cm gap between detector and patient (6.7 cm for hip examination). The 5 cm gap between patient and detector is due to e.g. the detector grid. In PCXMC the tube angle has to be defined at the point of rotation and the system that was used has the point of rotation 9.9 cm in front of the detector (11.6 cm for hip examination). The angles were recalculated from the clinical definition to the program definition using eq. 2, where  $\alpha_{PCXMC,i}$  is the angle that was used in the program and  $H_{0,i}$  is the absolute vertical distance the center of the x-ray tube have moved from the zero degree projection to the projection of interest.

$$\alpha_{PCXMC,i} = \tan^{-1}(H_{0,i}/(FDD - 9.9)) \quad \text{Eq. 2}$$

## Chest

The tomosynthesis system used for the simulations is the Definium 8000 with the tomosynthesis option VolumeRAD. For the scout image the system has a 180 cm FDD that increases to a maximum of 187 cm at the maximum angles at about  $\pm 15$  degrees. The exposure of the examination is determined by AEC of a scout image. The system has a fixed detector position while the tube moves vertically, acquiring 60 low-dose projection radiographs, and at the same time rotates so that the central ray of the x-ray beam always passes through a point located 9.9 cm in front of the detector plane. A constant tube load is used for each exposure, and the filtration typically used is 3.0 mm Al and 0.1 mm Cu.

The field of view used in the simulations for the scout image was determined by studying actual clinical scout images to see what anatomical parts were visible and using these anatomical markers to get accurate scout field of view. Definium 8000 system decreases the field height with larger angles. To replicate this change in height we used the geometrics of the examination as seen in fig. 3 where  $y_0$  is the field height at the zero degree projection,  $y_i$  is the field height at projection i and  $\alpha_i$  is the angle for projection i. From examination data the height of the field was found to decrease with increasing angles.

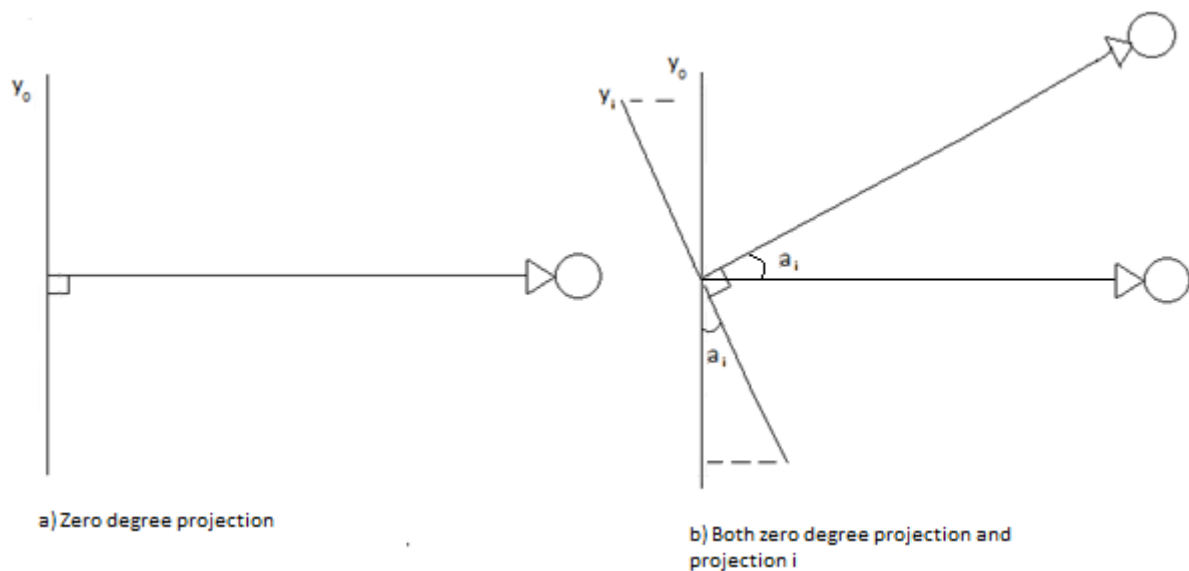


**Figure 3** The change of height in field size compared to the zero projection,  $\alpha$  is the projection angle,  $y_0$  the height of zero degree projection field,  $y_i$  the field height of the i projection

To be able to calculate the field height using the projection angle an empirically derived equation was found, see eq 3. The last term in eq. 3 is an expression for the magnitude of the cutoff section at the top of the field. The magnitude of this section is the same at the bottom and that is why the term is multiplied by two and subtracted from the field height at the zero projection.

$$\text{(Height)} \quad y_i = y_0 - 2 \times \frac{\frac{y_0}{2} \times \tan^2 \alpha_i}{(1 + \tan^2 \alpha_i)} \quad \text{Eq. 3}$$

(Width)  $x_i = x_0 \times k_i$  Eq. 4

From the data collected from an examination it was observed that the width of the field at the detector surface also changes. A conversion factor for the width of the field was calculated for each angle using the collected examination data. The value of  $k_i$  differed from 0,996 to 1,004. Field sizes that were calculated for the different angles were then compared to the examination data to see that they were accurate.

In the simulation of chest examination a variation of patient sizes was used. The variation was to include both a variation in patient weight and length, see table 2. For the standard sized patient (height 170 cm, weight 70 kg) the tube voltage was varied between 60 kVp and 150kVp. The relationship between KAP, mA s and effective dose was determined for each projection, patient size and tube voltage. Two types of conversion factors were then calculated one based on the total KAP used or by the mA s used. The total KAP or mA s used was determined by the examination data collected.

**Table 1 The patient sizes used in the Monte Carlo simulations and the corresponding field sizes at the detector surface for the zero degree projection**

BMI	Height (cm)	Weight (kg)	kV	Field Size WidthxHeight (cmxcm)
17.3	170	50	120	29x30
20.8	170	60	120	30.5x30.5
23.4	160	60	120	30x29
24.2	170	70	60-150	33x31
24.7	180	80	120	34x33
24.9	190	90	120	36x35
27.7	170	80	120	36x30.5
31.1	170	90	120	37x30.5
34.6	170	100	120	40x30.5

### Hip Joint

In the examination of the hip joints the same system is used, but since the patient in this examination is placed on a table top, this results in that the parameters differ from those of a chest examination. The FDD ranges from 100 cm to 107 cm at the maximum angles of  $\pm 20$  degrees. During the vertical movement acquiring the 60 low-dose projections the tube rotates so the center of the ray always passes through a point 11.6 cm in front of the detector plane. The difference in distance to the point of rotation from the detector compared with chest setup is due to the thickness of the table top.

For the hip simulation an examination of a hip phantom<sup>1</sup> was used to acquire data of the system field of view, angle, FDD and exposure. The examination was performed at the Sahlgrenska University

<sup>1</sup> Transparent Pelvis Phantom, RSD Model RS-113T, Gammex RMI, USA

hospital Mölndal with assistance from the orthopedic tomosynthesis specialist. The data for each projection was then used in PCXMC to calculate the effective dose. The summation of the projections then gave the total body effective dose of the tomosynthesis examination. The effective dose of the scout is equal to the dose from conventional 2-D radiograph. A conventional radiography examination of the hip joint can consist of between 1 to 3 2-D radiographic images.

## Results

The conversion factor for a chest tomosynthesis examination using the GE Definition 8000 system, using weighting factors from both ICRP 60 and ICRP 103, between KAP and effective dose as well as between mAs and effective dose, is presented in tables 3 and 4 for different patient sizes and tube voltages. Table 3 presents the conversion factors for different patient sizes calculated with a tube voltage of 120 kV. The conversion factors based on KAP decreased with increasing patient weight. The conversion factor based on mAs also showed a general decrease with increasing patient weight, but the dependency was much weaker. Figure 4 shows the  $E_{KAP}$  conversion factor, according to ICRP 103, as a function of the patient weight for a 170 cm patient.

**Table 2** The conversion factors between KAP and effective dose and between mAs and effective dose, using weighting factors from both ICRP 60 and ICRP 103 for a chest tomosynthesis examination using the GE Definition 8000 system for patients of different sizes at a tube voltage of 120 kV.

Height(cm)/ Weight(kg)	$E_{KAP}$	$E_{KAP}$	$E_{mAs}$	$E_{mAs}$
	mSv Gy <sup>-1</sup> cm <sup>-2</sup> ICRP 60	mSv Gy <sup>-1</sup> cm <sup>-2</sup> ICRP 103	mSv mA <sup>-1</sup> s <sup>-1</sup> ICRP 60	mSv mA <sup>-1</sup> s <sup>-1</sup> ICRP 103
170/50	0.350	0.386	0.00597	0.00658
170/60	0.311	0.340	0.00567	0.00620
160/60	0.311	0.338	0.00530	0.00576
170/70	0.276	0.299	0.00553	0.00598
180/80	0.247	0.266	0.00542	0.00584
190/90	0.220	0.236	0.00541	0.00582
170/80	0.245	0.264	0.00528	0.00568
170/90	0.226	0.241	0.00485	0.00518
170/100	0.204	0.217	0.00487	0.00518

Conversion factors for KAP for a patient sized 170 cm and 70 kg (BMI 24.2), simulated for chest examination using different tube voltages, is presented in table 4. With increasing tube voltage the conversion factor increased from 0.162 mSv Gy<sup>-1</sup> cm<sup>-2</sup> for 60 kV to 0.326 mSv Gy<sup>-1</sup> cm<sup>-2</sup> for 150 kV using ICRP 103.

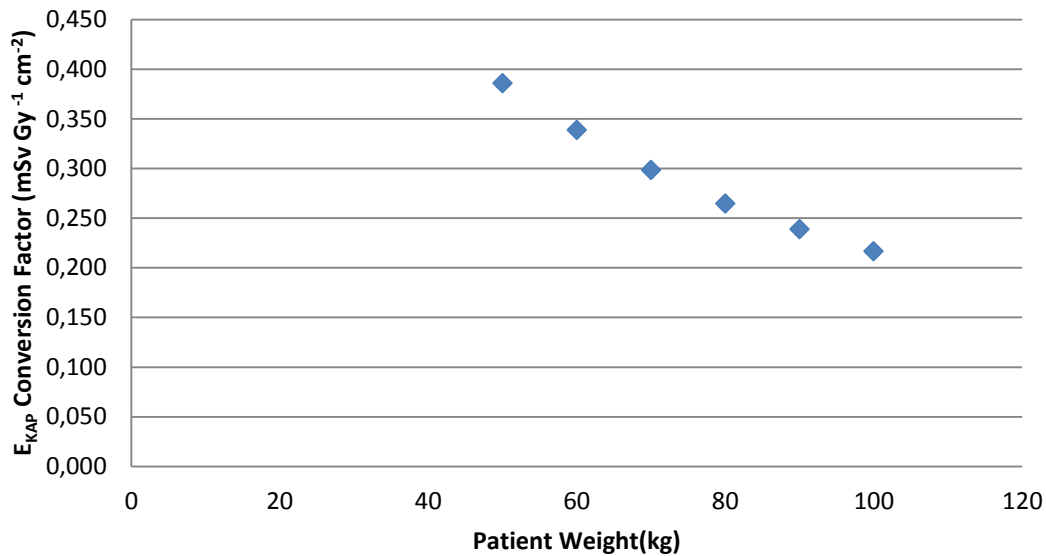


Figure 4 The  $E_{KAP}$  conversion factor according to ICRP 103 as a function of the patient weight for a 170 cm patient.

The effective dose for the hip joint examination was found to be 0.86 mSv for ICRP 103 and 1.19 mSv for ICRP 60. The dose of a conventional AP radiograph was found to be 0.09 mSv. The average  $E_{KAP}$  conversion factor for the same examination was 0.102  $mSv Gy^{-1} cm^{-2}$  for ICRP 103 and 0.141  $mSv Gy^{-1} cm^{-2}$  for ICRP 60.

Table 3 The conversion factors between KAP and effective dose and between mA s and effective dose, using weighting factors from both ICRP 60 and ICRP 103 for a chest tomosynthesis examination using the GE Definition 8000 system at different tube voltages for a standard patient (170 cm, 70 kg).

kV	$E_{KAP}$	$E_{KAP}$	Relative difference to 120kV (%)
	$mSv Gy^{-1} cm^{-2}$ ICRP 60	$mSv Gy^{-1} cm^{-2}$ ICRP 103	
60	0.153	0.162	-46%
70	0.183	0.195	-35%
80	0.210	0.225	-25%
90	0.232	0.250	-16%
100	0.250	0.269	-10%
110	0.265	0.285	-4%
120	0.276	0.299	0
130	0.286	0.309	+3%
140	0.295	0.317	+6%
150	0.301	0.326	+9%

## Discussion

It is clear that the average conversion factors between KAP and effective dose are affected by both patient size and tube voltage, as shown in table 2 and 3. For patients of the same height, the decreased conversion factor for patients with larger weight, which can be seen in table 3, is mainly caused by the fact that the ratio between mean absorbed dose and entrance dose is smaller for

larger patients. The decrease is also due to the increase in field size. Also for patients with similar BMI but different size, smaller patients have a higher conversion factor than larger patients. This is partly due to the difference in field of view. The weak dependency on patient size for the conversion factor to effective dose from mAs compared to KAP shows that mAs may be a better universal conversion factor for all patient sizes than KAP. However using mAs instead of KAP means that the filter also has to be known exactly. So in practicality the KAP conversion factor might still be the simplest to use. The large difference in conversion factors between different patient sizes, ranging from  $0.386 \text{ mSv Gy}^{-1} \text{ cm}^{-2}$  for the thinnest patient to  $0.217 \text{ mSv Gy}^{-1} \text{ cm}^{-2}$  for the most obese, leads to the conclusion that there is a dependency on patient size for the conversion factor for KAP.

There is a clear dependency on tube voltage for the conversion factor, as can be seen in table 4. The higher the tube voltage the higher the conversion factor and the reason for this is that a higher tube voltage will result in a larger ratio between mean absorbed dose and entrance dose when the patient size is kept constant. What can also be seen is that the difference in percent from the conversion factor for 120 kV is larger for lower tube voltages than for higher tube voltages.

The present work is limited in the sense that it is confined to the clinically used system Definium 8000 VolumeRAD, which has a fixed detector and a vertical motion of the X-ray tube. What values other systems that have both a mobile detector and X-ray tube would generate in comparison is not possible to predict, nor can it be predicted if they will ever be introduced clinically. However, a similar but still more general system compared to that of Definium 8000 VolumeRAD was investigated by Svalkvist et al. (20) The differences between this general system and the Definium 8000 VolumeRAD system was that in the previous the pivot point was located at the detector surface, the distribution of the projections was uniform over the angular interval and the field size was constant at the detector surface for all projections. The conversion factors in the paper by Svalkvist et al. (20) for different patient sizes was smaller than those presented in this paper, except for the patient with a BMI of 23.4, and the same patient sizes were used in both papers. The difference in conversion factor ranged from  $0.0137 \text{ mSv Gy}^{-1} \text{ cm}^{-2}$  lower than present work for the patient with a BMI 24.2, to being  $0.00108 \text{ mSv Gy}^{-1} \text{ cm}^{-2}$  higher for the patient with a BMI of 23.4. The average difference is  $0.0105 \text{ mSv Gy}^{-1} \text{ cm}^{-2}$  lower than the present work, which gives a difference of 3.8 %. When the conversion factors for different tube voltages are compared, the current paper also has higher conversion factors in general. The biggest difference is  $0.0149 \text{ mSv Gy}^{-1} \text{ cm}^{-2}$  for a tube voltage of 150 kV and the average difference is  $0.0127 \text{ mSv Gy}^{-1} \text{ cm}^{-2}$ . The difference does not increase or decrease with the tube voltage, so the reason for differences could be the same as in the case of the patient sizes. In a paper by Båth et al. (20) the conversion factor was found to be  $0.26 \text{ mSv Gy}^{-1} \text{ cm}^{-2}$  for a patient size of 170.9 cm 70.2 kg, corresponding to the patient with a BMI 24.2 in the present paper, which had a conversion factor of  $0.299 \text{ mSv Gy}^{-1} \text{ cm}^{-2}$ . In the paper by Båth et al. the same system was used as in the present paper, and was also based on real examinations, the difference however can somewhat be caused by different field placement. These differences may not appear much, but it is a significant difference and the reasons can be hard to determine due to multiple variables. The field sizes used at the zero degree projection is in general slightly larger in this paper than in Svalkvist et al. (21), but based on this the expectation would be that the conversion factors of Svalkvist's study should have been higher, which was not found to be the case. The differences in the systems discernibly affect the conversion factors, even though the systems are very similar but the reason for higher values in the present paper could be from how the field is placed. If thyroids are in field of view the conversion factors will be higher and in this paper they

were. It is not clear if the thyroids were in the field of view in the paper presented by Svalkvist et al or Båth et al. To get away from these differences an examination standard protocol where it is determined what organs should or should not be part of field of view should be set.

The sources of error in this paper partly derive from the statistical error in the Monte Carlo simulation. This error was  $<0.1\%$  in the present study, and could have been decreased further by using more photon histories, but the extended time this would add to the simulations would make it very impractical. There is also a small error in the way that the field of view changes with the angle. The simulated field size and the actual field size could differ with about  $\pm 0.01$  cm, with the error in percent being about  $0.1\%$ . Both these errors however are very small in comparison to the uncertainties of the field sizes chosen, which in a clinical situation can differ greatly between operators and the objective of the examination. It is common that field sizes are smaller in simulations compared to clinical examinations, even if, as in this paper, actual examination images have been used as guides to select a correct size. To which extent this can affect the conversion factor is hard to predict, but it could be as high as  $10\%$ , as can be seen when comparing the present study to Båth et al. (20). When choosing a field of view, it is not only the actual field size that matters, but also how the field is placed. This can also have a substantial effect on the conversion factor, with the crucial point being how much of the neck is within the field of view. More precisely, if the thyroids are partly or completely in the field of view it could have an effect, since the thyroid is one of the more radiosensitive organs in the body. Some of the images used as guides to determine the place and size of the field featured thyroids even though it looked as though they could be excluded and still have all of lungs in the picture. However if this is possible to tell before the examination is done or true for all bodies is not able to tell

In the present paper the effective dose of a hip joint tomosynthesis was found to be  $0.86$  mSv. This is quite high in comparison to a chest tomosynthesis which is about  $0.13$  mSv, although about the same amount of radiosensitive organs are present in a hip examination and in a chest examination. In a hip examination however a higher KAP is needed than in a chest exam, due to the much higher attenuation in this body region.

Conventional 2-D radiography of the hip joint was determined to be  $0.09$  mSv. This means that a tomosynthesis gives about 9.5 times higher dose than the conventional radiography. However if a hip examination is made with 2 or 3 2-D images the effective dose is only about 5 or 3 times greater in a tomosynthesis. As mentioned earlier the effective doses are generally quite high, but can be lowered simply by restricting the field of view to the hip joint. This way the dose would probably be greatly diminished. If both hip joints are of interest it might be better to do one tomosynthesis of each individual hip joint rather than one of both. However, a conclusion whether this would actually lower the dose is cannot be drawn from these results and further research into the field is needed.

## Conclusion

In conclusion the conversion factor between KAP and effective dose for a chest tomosynthesis examination using the GE Definium 8000 system changes with both patient size and tube voltage, and using a singular conversion factor for all would generate large errors in the dose estimation. For patients with the same height ( $170$  cm), the conversion factor decreases with increasing patient weight from  $0.386$  mSv  $\text{Gy}^{-1} \text{cm}^{-2}$  for a  $50$  kg patient to  $0.217$  mSv  $\text{Gy}^{-1} \text{cm}^{-2}$  for a  $100$  kg patient at a

tube voltage of 120 kV. For a standard patient (170 cm, 70 kg), the conversion factor increases with increasing tube voltage from 0.162 mSv Gy<sup>-1</sup> at 60 kV cm<sup>-2</sup> to 0.326 mSv Gy<sup>-1</sup> cm<sup>-2</sup> at 150 kV. A tomosynthesis examination of the hip joint for a standard size patient gives an effective dose of 0.86 mSv which is about a 9.5 times higher effective dose than that of a single conventional AP radiography.

## Acknowledgements

I would like to thank my supervisors Magnus Båth and Angelica Svalkvist for all their help. I also want to thank Sahlgrenska University hospital Mölndal for all the help with the hip joint examination. A big thank you to Stina Larsson for all the help with grammar, spellchecking and layout. Last I want to thank Skilla for the moral support and companionship during this paper.

## References

1. A. Svalkvist, *Development of Methods for Evaluation and Optimization of Chest Tomosynthesis*, Institute of Clinical Sciences at Sahlgrenska Academy, University of Gothenburg (2011)
2. J. T. Dobbins III, H. P. McAdams, D. J. Godfrey, and C. M. Li, *Digital Tomosynthesis of the chest*, Thorax Imaging Vol 23, **2**, 86-92 (2008)
3. J. T. Dobbins III, *Tomosynthesis imaging: At a translational crossroads*, Med. Phys. **36**, 1956-1967 (2009)
4. J. T. Dobbins III, H. P. McAdams, *Chest tomosynthesis: Technical Principles and clinical update*, European Journal of Radiology, **72**, 244-251 (2009)
5. B.G. Ziedses des plantes, *Eine neue method zur differenzierung in der roentgenographie (planigraphie)*, Acta Radiol. **13**, 182-192 (1932).
6. D. G. Grant, *Tomosynthesis: A three-dimensional radiographic imaging technique*, IEEE Trans. Biomed. Eng. **BME-19**, 20-28 (1972).
7. D.N. Ghosh Roy, R.A Kruger, B. Yih, and P. Del Rio, *Selective plane removal in limited angle tomographic imaging*, Med. Phys. **12**, 65-70 (1985).
8. D.P. Chakraborty, M. V. Yester, G. T. Batnes, and A. V. Lakshminarayanan, *Self-masking subtraction tomosynthesis*, Radiology **150**, 225-229 (1984)
9. J. T. Dobbins III, H. P. McAdams, J.-W. Song, C. M. Li, D. J. Godfrey, D. M. DeLong, S.-H. Paik, and S. Martinez-Jimenez, *Digital tomosynthesis for the chest for lung nodule detection: Interim sensitivity results from an ongoing NIH-sponsored trail*, Med. Phys. **35**, 2554-2557 (2008)
10. P. Edholm, G. Granlund, H. Knutsson, and C. Petersson, *Ectomography: a new radiographic method for reproducing a selected slice of varying thickness*, Acta Radiol. **21**, 42-433 (1980)
11. K. R. Maravilla, R. C. Jr Murry, and S. Horner, *Digital tomosynthesis: technique for electronic reconstructive tomography*, American Journal of Roentgenology, **141**, 497-502 (1983)
12. R. A. Kruger, M. Sedaghati, and D. G. Roy, *Tomosynthesis applied to digital subtraction angiography*, Radiology **152**, 8-805 (1985)
13. R. Vandre, R. Webber, R. Horton, C. Cruz, and J. Pajak, *Comparison of Tact with film for detecting osseous Jaw lesions*, Journal of dental research **74**, 18 (1995)

14. J. Duryea, J. T. Dobbins III, and J. A. Lynch, *Digital tomosynthesis of hand joints for arthritis assessment*, Med. Phys. **30**, 33-325 (2003)
15. M. J. Flynn, R. McGee, and J. Blechinger, *Spatial resolution of X-ray tomosynthesis in relation to computed tomography for coronal/sagittal images of the knee*, Proceedings of SPIE **6510**, 0D1-D9 (2207)
16. T. Wu, A. Stewart, and M. Stanton, *Tomographic mammography using a limited number of low-dose cone-beam projection images*, Med. Phys. **30**, 80-365 (2003)
17. J. T. Dobbins III, H. P. McAdams, and J.-W. Song, *Digital tomosynthesis of the chest for lung nodule detection: interim sensitivity results from an ongoing NIH-sponsored trial*, Med. Phys. **35**, 7-2554 (2008)
18. D. J. Godfrey, H. P. McAdams, and J. T. Dobbins III, *Optimization of the matrix inversion tomosynthesis (MITS) impulse response and modulation transfer function characteristics for chest imaging*, Med. Phys. **33**, 655-67 (2006)
19. U. E. Ruttimann, R. A. J. Groenhuis, and R. L. Webber, *Restoration of digital multiplane tomosynthesis by a constrained iteration method*, IEEE Transactions on Medical Imaging, **3**, 141-148 (1984)
20. M. Båth, A. Svalkvist, A. von Wrangel, H. Rismyhr-Olsson, and Å. Cederblad, *Effective dose to patients from chest examinations with tomosynthesis*, Radiation Protection Dosimetry Vol. 139, **1-3**, 153-158 (2010)
21. A. Svalkvist, L. G. Månsson, and M. Båth, *Monte Carlo Simulations of the dosimetry of chest tomosynthesis*, Radiation Protection Dosimetry Vol. 139, **1-3**, 144-152 (2010)
22. ICRP. *The 2007 Recommendations of the International Commission on Radiological Protection*. ICRP Publication 103 (Oxford: Pergamon press) (2007)
23. ICRP. *The 1990 Recommendations of the International Commission on Radiological Protection*. ICRP Publication 60 (Oxford: Pergamon press) (1991)
24. M. Tapiovaara, and T. Siiskonen, *PCXMC-a Monte Carlo program for calculating patient doses in medical X-ray examinations*, second edn. STUK-A23, Helsinki, Finland:STUK (2008)
25. J. M. Sabol, *A Monte Carlo Estimation of effective dose in chest tomosynthesis*, Med. Phys. **36**, 5480-5487 (2009)
26. [www.icrp.org](http://www.icrp.org)